Journal of Materials Chemistry B

Accepted Manuscript

ROYAL SOCIETY OF CHEMISTRY

www.rsc.org/materialsB

Self-programmed nanovesicle to nanofiber transformation of a dipeptide appended bolaamphiphile and it's dose dependent cytotoxic behaviour

Indrajit Maity,[a] Hamendra S. Parmar,[b] Dnyaneshwar B. Rasale,[a] and Apurba K. Das*[a]

Abstract: Nanostructural transition of a small peptide bolaamphiphile via molecular self-assembly is a challenging task. Here, we report self-programmed morphological transformation from nanovesicles to nanofibers of a smart peptide bolaamphiphile in it's self-assembling hydrogel state. The nanostructural transition occurs based on the structural continuity of the β-sheet structures. The spectroscopic studies confirmed different molecular arrangements of two different nanostructures. Furthermore, the smart bolaamphiphile shows dose dependent cytotoxicity and cell-proliferation behaviour.

1. Introduction

Precise control in nanostructural transition of small peptide based bolaamphiphile molecules via molecular self-assembly is a challenging task. Peptide based nanostructures[1-10] are envisaged through bottom up self-assembly approach,[11-15] which possess wide range of applications in drug delivery,[16-19] tissue engineering[20-25] and supramolecular electronics.[26-28] However, peptide self-assembly process are highly sensitive towards change in stimuli like pH,[29-31] temperature,[32,33] light,[34] metal ions[35,36] and enzymes.[37-40] Delicate hydrophobic / hydrophilic balance and non-covalent interactions of a molecule are the driving force for the self-assembly process in a particular solvent, which results in the formation of peptide nanostructures. Stimuli responsive peptide self-assembly proceeds through alteration of molecular conformations, which lead to adopt different secondary structures. The self-assembly process is dynamic in nature. The dynamic behaviour acts in between the more and relatively less ordered conformational arrangements at molecular level. Nanostructural transition occurs owing to achieve a more stable and ordered molecular arrangement from the loosely ordered arrangement in a particular system.

Most of the cases, change in stimuli directs the morphological transformation from one nanostructure to another nanostructure. Stimuli responsive peptide nanofibers have drawn attention due to their potential applications in drug delivery and waste water treatment.[41] Nanostructural transition of peptide into tapes, ribbons, nanofibrils and nanofibers depends on change in pH.[42] Parquette *et al.* reported peptide based dendron self-assembly in a controlled manner and interconversion of nanotubes and fibrillar nanostructures.[43] Direct morphological transformation from twisted ribbons to helical ribbons was reported by Stupp *et al*.[44] Ulijn group reported morphological transformation from a micellar solution to a fibrous hydrogel via enzymatic dephosphorylation of a peptide amphiphile.[45] Again, the same group demonstrated direct enzymatic amide condensation and light induced controlled gelation, which is associated with morphological transition from micellar structure to entangled nanofibers.[46] Yang *et al.* tuned the hydrogelation process by enzymatic dephosphorylation of a small molecule and found morphological transformation.[47]

Peptide bolaamphiphiles are interesting class of organic molecules. In a bolaamphiphile molecule, two terminal hydrophilic groups are attached with a hydrophobic backbone. Shimizu *et al.* demonstrated various types of nanostructure forming peptide bolaamphiphiles.[48] Nano-doughnut forming self-assembled peptide bolaamphiphile was also used as a nanoreactor to synthesis Au nanocrystal.[49] The nanostructural transformation requires a stimulus, which can break weak non-covalent interactions and induces another supramolecular arrangement. The change in pH can tune the evolution of different nanostructures of bolaamphiphiles.[50] Here, we report self-programmed morphological transition from nanovesicles to nanofibers via a third polymorphic state of nanocapsules.

Cytotoxic study of small molecules has emerged a promising tool which leads to the technological innovation for the development of drugs.[51] Understanding the dose dependent behavior of a small molecule is crucial and important aspect in the field of biomedicine.[52,53] Hydrogels of small peptide based molecules are interesting due to their applications in cell-biology.[54] The objectives of this paper are (a) to incorporate a flexible alkane chain which can give different structures due to conformational heterogeneity, (b) to study the nanostructural transition driven by molecular self-assembly, (c) to understand the mechanism of the

nanostructural transition with respect to time and (d) to investigate the cytotoxicity and cell proliferation using the self-assembled hydrogel scaffold.

2. Experimental

2.1 Preparation of hydrogel:

15 mg (10 mmol L^{-1}) of peptide bolaamphiphile (HO-W-F-Suc-L-W-OH) was dispersed in 2 mL of sodium phosphate buffer solution (pH 8, 10 mmol L^{-1}) and sonicated for 10 minutes. It was found that the self-supporting hydrogel was formed after 3 hours.

2.2 General characterization:

All NMR characterizations were carried out on a Bruker AV 400 MHz spectrometer at 300 K. Compound concentrations were in the range 5-10 mmol in $(CD_3)_2SO$ and $CDCl_3$. Mass spectra were recorded on a Bruker micrOTOF-Q II by positive mode electrospray ionisation. Specific rotations of the synthesized compounds were measured on an Autopol V automatic polarimeter (Rudolph Research Analytical). The cell (length = 100 mm, capacity = 2 mL) was used for this study at 20 °C. For AFM study, the gel samples were diluted in Milli Q water to a final concentration of 0.5 mmol L^{-1} and placed on a mica slip. Then, it was dried by slow evaporation. Images were taken with AIST-NT instrument (model no smartSPM 1000) using soft tapping-mode. FT-IR spectra for both the nanovesicles and nanofibers were taken using Bruker (Tensor 27) FT-IR spectrophotometer. The gel sample was prepared in D_2O and placed between crystal Zn-Se windows and scanned between 900 to 4000 cm^{-1} over 64 scans at a resolution of 4 cm^{-1} and an interval of 1 cm^{-1}. Secondary structure of peptide bolaamphiphile was analyzed with Jasco J-815 circular dischroism spectrometer. The peptide hydrogel (10 mmol L^{-1}) was diluted to a final concentration of 500 μM in ddH_2O for both the vesicles and nanofibers and measured from 280 nm to 190 nm with 0.1 data pitch, 20 nm min^{-1} scanning speed, 1 nm band width and 4 s D.I.T. Fluorescence emission spectra of hydrogel (10 mmol L^{-1}) for both the states of nanovesicles and nanofibers were recorded on a Horiba Scientific Fluoromax-4 spectrophotometer with 1 cm path length quartz cell at room temperature. The slit width for the excitation and emission was set at 2 nm and a 1 nm data pitch. Excitation of gel sample was performed at 280 nm and data range was in between 290 to 500 nm. Data were collected for both

the nanostructures of nanovesicles and nanofibers on a Rigaku Smart Lab X-ray diffractometer with a wavelength of 1.5406 Å. The X-rays were produced using a sealed tube and the X-rays were detected using a linear counting detector based on silicon strip technology (Scintillator NaI photomultiplier detector). Fluorescence microscopy experiments were performed on a home-built epifluorescence microscopy setup. An air-cooled argon ion laser (Melles Griot, model 400-A03) with excitation wavelength at 500 nm was used to excite the vesicle sample placed on an inverted microscope (Nikon, model Eclipse Ti-U). The laser beam was expanded and subsequently focused on the back-focal plane of an oil immersion objective (100 × 1.49 NA Nikon) to illuminate 60 × 60 μm^2 area of the sample. The PL from the sample was collected through a B2A filter cube (Nikon) with a 505 nm dichroic mirror and a 520 nm long-pass filter and finally imaged with a back-illuminated EMCCD camera (Andor, model iXon X3 897). The exposure time was 300 ms. The images were analyzed with ImageJ (Version 1.46r) NIH. Optical microscopy images were taking with a Zeiss AxioCam ERc5s microscope using 40X magnification. The peptide bolaamphiphile vesicles and Congo red loaded vesicles were diluted in double distilled water and the samples were prepared by depositing a few drops on a cover slip.

2.3 Cell culture (MTT assay): Total WBCs were isolated from chicken blood. The 1 x 10^6 / mL concentration of cells was taken 100 µL in each well. 20 mmol L^{-1} concentration of hydrogel stock solution was used to prepare resulting concentrations of 10 - 100% in different wells (each in triplicate) at a pH of 7.4. Commercially available kit from Hi-Media Pvt. Ltd., Mumbai was used to conduct MTT assay. Cells were mixed with the hydrogel and incubated for 48 hours with the hydrogel or in media (control). Minimum essential media without phenol red was used to culture the cells. After culturing the cells, the MTT reagent was added to each well. After 4 h, the MTT solution was carefully removed and the purple crystals were solubilized in DMSO. The optical density of the reagent was then measured at a wavelength of 570 nm with a reference wavelength of 650 nm. Effect on cell viability or number was calculated in percentage considering the average absorbance value from control samples as 100%.

2.4 Statistical Analysis:

Data are expressed as mean ± SEM and were analyzed by the analysis of variance (ANOVA) followed by a post hoc Newman-Keuls Multiple Comparison Test using a trial version of Prism 5 software for Windows (GraphPad Software, Inc., La Jolla, CA, USA).

3. Results and discussion

We have synthesized a peptide bolaamphiphile HO-W-F-Suc-L-W-OH (W: Tryptophan, L: Leucine, F: Phenylalanine and Suc: Succinic acid) with a centrally located flexible succinic acid moiety. 15 mg of peptide bolaamphiphile (10 mmol L^{-1}) was dispersed in 2 mL of phosphate buffer (pH = 8, 10 mM). A self-supporting hydrogel was achieved by successive sonication which was subjected to investigate the morphological transformation (Scheme 1). The critical gelation concentration of the precursor was found as 8 mmol L^{-1}. The self-programmed nanostructural transition from nanovesicle to nanofiber of hydrogel **1** (10 mmol L^{-1}) with self-assembly mechanism with respect to time was studied by transmission electron microscopy (TEM) and atomic force microscopy (AFM).

Transmission electron microscopy image (Fig. 1) showed that the peptide bolaamphiphile self-assembled to form nanovesicles within 5 hours of hydrogelation. At this early stage, the evolution of nanovesicles[55] occured through loose molecular arrangement of self-assembled molecules (ESI,† Fig. 1). TEM image revealed the average diameter of the nanovesicles is 48 nm. The average wall thickness of these nanovesicles is 3.7 nm (Scheme 1). At day 1, the TEM image showed that the early evolved nanovesicles become larger in size and the average diameter was observed as 290 nm. The average wall thickness was estimated from the TEM image, which was observed as 15 nm. The vesicle-wall was formed by multilamellar arrangement of self-assembled molecules, which adopted a loose β-sheet like structure. At day 2, nanocapsule like nanostructure was observed with increased in dimension. The length of the capsule was about 1.35 μm and the diameter was around 500 nm at the middle of the nanostructure. At this stage, association of two or more nanovesicles was also observed. It is evident that the nanocapsule like nanostructure was evolved from the association of the nanovesicles (Fig. 2). The nanofibrillar structures[31] were observed after 4 days of hydrogelation.

The TEM image showed that the nanofibrillar network structures were formed from previous collapsed nanostructure and the nucleation point was clearly observed in the TEM image. The nanofibers were several micrometer in length and the average diameter of the nanofiber was 2 nm. At this stage, no nanovesicle was found which indicates the complete conversion of nanovesicles to nanofibers (ESI,† Fig. 2).

The atomic force microscopy (AFM) images[56,57] (Fig. 3) were also similar in trend with the TEM images. The peptide bolaamphiphile molecules self-assembled into nanovesicles at early stage. The size of nanovesicles at 5 hours of hydrogelation was in the range of 45 to 150 nm. After that, the nanovesicles were fused with each other to form cocoon like nanostructures. The average diameter of these nanostructures was 300 nm. At 2 days of self-assembly, the cocoon like nanostructures transformed into nanocapsule like structures which were 0.6 to 1.3 μm in length. The average diameter of these nanocapsules was 500 nm and the height was in the range of 5 to 10 nm (ESI,† Fig.3). At 5 days of sonication, nanofibers were formed. The diameter of the nanofiber was 20 nm. The self-assembly process was initiated by sonication but the morphological transition from nanovesicles to nanofibers occurred by self-programmed process of smart bolaamphiphile.

The hollow nature of the nanovesicles was proved by Congo red dye encapsulation experiment.[58] An aqueous solution (2 mg mL^{-1}) of the Congo red dye was prepared and added into the vesicles. These vesicles entrapped Congo red dye within a period of 4-5 hours. After 5 hours, the fluorescence microscopic images (Fig. 4) clearly demonstrated that the physiological dye, Congo red, is successfully encapsulated inside the vesicles. In addition with the fluorescence microscopic images, the optical microscopy images[59] also showed the vesicle structures of the peptide bolaamphiphile hydrogel at 1 day of self-assembly (ESI,† Fig. 4).

From the above observations, we were interested to elucidate the differences in the molecular arrangement in supramolecular level inside these two different nanostructures. To get insight about the molecular conformations of two different nanostructures, several spectroscopic analyses were performed. FTIR study was carried out at day 1 and 5 of hydrogelation to

understand the secondary structures adopted by the self-assembled peptide bolaamphiphiles inside the two different nanostructures. At day 1, two peaks appeared at 1646 cm^{-1} and 1714 cm^{-1} for the hydrogel enrich with nanovesicles. The peak at 1714 cm^{-1} suggested that the carboxylic acid groups are involved in hydrogen bonding interactions whereas the appearance of characteristic amide I peak at 1646 cm^{-1} revealed turn type of β-sheet arrangement.[60] At day 5, several characteristics peaks appeared for the hydrogel consisting the nanofibrillar morphology. The C=O stretching band at 1702 cm^{-1} was indicated for the hydrogen bonded carboxylic acid functionality in the peptide nanofibers. The amide I band at 1635 cm^{-1} along with a weak shoulder at 1608 cm^{-1} revealed that the peptide bolaamphiphile molecules are self-assembled into hydrogen bonded β-sheet arrangement[9] in the nanofibers (Fig. 5a). From the FTIR spectra, it is clear that the molecular packing is more ordered and more compact into the β-sheet arrangement for the nanofibers rather than the nanovesicles.

The difference in the molecular conformations inside the two different nanostructures at two different stages of self-assembly was examined by circular dichroism (CD) spectroscopy (Fig. 5b).[61,62] For both the cases, the hydrogels were diluted to 500 μM concentration in dd H_2O to investigate the secondary structures for two different nanostructures. The CD spectrum for nanovesicles showed a characteristic negative peak around 201 nm with a weak shoulder at 211 nm which are resulted from the n-π* transition of the CO-NH groups of the peptide bolaamphiphile molecule. This CD signature represented a coil-type β-sheet arrangement of peptide bolaamphiphiles in the nanovesicle. Another strong positive band appeared at 226 nm, which is responsible for the electron-transfer of the nonbonding electron of the nitrogen atom into the π* orbital system of the indole ring of the tryptophan moiety.[63] The CD spectrum for the nanofibers showed the characteristic negative band at 216 nm with a weak negative band at 201 nm for n-π* transition of the CO-NH groups. This CD signature confirmed the hydrogen bonded β-sheet arrangement, which is more ordered for nanofibers rather than nanovesicles. The other positive band at 229 nm was appeared for tryptophan moiety which is slightly red shifted with increase in ellipticity from the corresponding peak of nanovesicles. This occured from the extended π-π stacking interactions of tryptophan aromatic rings during the self-assembly process to form nanofibers.

Fluorescence spectroscopy technique was also exploited to explore π-π stacking interactions during self-assembly process of peptide bolaamphiphile and to understand the role of aromatic moieties of peptide bolaamphiphile during structural transition from nanovesicles to nanofibers (Fig. 5c). Fluorescence spectra showed that the nanovesicles emitted at 353 nm whereas the nanofibers give emission maxima at 357 nm upon the excitation of 280 nm. The emission peak for both the cases was resulted from the tryptophan moiety of self-assembled bolaamphiphile molecules. The 4 nm red shift of emission maxima occurred from the naostructural transition of nanovesicles to nanofibers which suggest that the peptide bolaamphiphiles are arranged into more ordered and compact β-sheet structures through the synergic effects of hydrogen bonding and extended π-π stacking interactions of the tryptophan residues inside the nanofibers.[9]

The powder X-ray diffraction (PXRD) data (Fig. 5d) clearly revealed the conformational differences between two morphological states of nanovesicles and nanofibers. For nanovesicles, the characteristic peak at 2θ = 18.96° corresponding to d spacing of 4.67 Å was observed. The peak at 4.67 Å is related to the spacing between two peptide bolaamphiphiles in a β-sheet arrangement.[64] For the nanofibers, a signal at 2θ = 20.15° corresponding to the d spacing of 4.40 Å, was observed which is related to the spacing between two successive peptide backbones in a β-sheet arrangement. In addition, several reflections were observed in the 2θ range of 4-11°, which are resulted from the ordered stacking periodicity of a β-sheet.[55] The typical peak at 2θ = 10.31° corresponding to d spacing of 8.56 Å revealed the distance between two successive β-sheets. The powder X-ray diffraction data clearly demonstrated that the peptide bolaamphiphiles are self-assembled into more ordered β-sheet arrangement inside the nanofibers rather than the nanovesicles.

To get the more structural information, the hydrogel at two different states was characterized by ^{1}H and 2D NMR spectroscopy. Nanovesicles and nanofibers enriched hydrogels were lyophilized and characterized by NMR in DMSO-d6 (ESI,† Fig. 8-13). All the ^{1}H NMR, ^{1}H-^{1}H COSY and ROESY spectra showed similar patterns for both the nanovesicle and nanofiber states. The ROESY spectra (ESI,† Fig. 11 and 13) for both the states showed that the tryptophan amide -CONH- protons are interacting with the -CH_2- protons of succinic moiety. The NMR results demonstrated the twisting conformation of self-assembled peptide bolaamphiphile in the

hydrogel phase for both the nanostructures. Here, we proposed a mechanism of self-assembly process, which formulated the nanostructural transition from nanovesicles to nanofibers. Fig. 1d revealed a schematic representation for morphological transformation. At early stage, self-assembly process leads to the formation of β-sheets, which form curved sheet by higher ordered self-assembly. Two-dimensional curved sheets result in the formation of nanovesicle structures.[65] After 4 days, nanofibrous morphology is formed via reorientation of stable β-sheet structures.

The cellular toxicity and proliferation studies with peptide based materials made an upward research interest in the field of biomedicine and biotechnology.[66,67] We investigated the cytotoxic and biocompatible behaviour with the cell proliferation of this peptide bolaamphiphile. To achieve a conclusion, we have cultured the WBC (white blood corpuscle) cell with different concentration of hydrogel. Total WBCs were isolated from chicken blood. 20 mmol L^{-1} concentration of hydrogel stock solution was used to prepare the resulting concentrations of 10-100% in different wells (each in triplicate). Cells were incubated for 48 hours with the hydrogel solution and in media for control experiment. Minimum essential media without phenol red was used to culture the cells. Effect on cell viability was calculated in percentage considering the average absorbance value from control samples as 100%. Data from Table 1 shows that the cell viability and cell proliferation occurred at 40 and 50% hydrogel concentration but maximum increase in cell viability was found at 50% concentration of hydrogel solution. The 30% concentration of hydrogel solution seemed to be safe but rest of the concentrations are found to be either suboptimal to exert any substantial effects or toxic (at higher doses). Data from MTT assay (ESI) consistently revealed the dose dependency of the used hydrogel as the best effect which was observed at 50% media supplementation by hydrogel. Lower concentrations are proved to be lesser effective and higher concentrations are found to be toxic in nature. Replacement of 50% culture media by hydrogel becomes most effective for proliferation. Cell viability suggested that the use of hydrogel along with media may be suitable to prevent from toxicity and to increase viability and cell growth. Similar effects on cellular viability and membrane fluidity were also observed earlier in case of drug compound and herbal extracts.[68-70]

4. Conclusions

In summary, we describe sonication induced phenylalanine and tryptophan rich peptide bolaamphiphile self-assembly through the synergistic effects of H-bonding and π-π stacking interactions. The self-assembling peptide bolaamphiphiles form self-supporting nanostructured fluorescent hydrogel. The self-programmed nanostructural transition from nanovesicles to nanofibers of peptide bolaamphiphiles occurs through structural continuity of stable β-sheets. The real time nanostructural transition was examined by TEM and AFM. The molecular confomations and arrangements for both the cases are investigated thoroughly by using various spectroscopic techniques. The spectroscopic studies suggest loose β-sheet arrangements of peptide bolaamphiphiles inside the vesicles. Moreover, peptide bolaamphiphiles are self-assembled into more ordered and compact β-sheet arrangement inside the nanofibers. Further more, the peptide bolaamphiphile shows dose dependent cytotoxic and cell proliferation behaviour.

Acknowledgements

AKD would like to acknowledge CSIR, New Delhi, India for financial support. IM and DBR are indebted to CSIR, New Delhi, India for their fellowship for this work.

Notes and references

[a] *Department of Chemistry, Indian Institute of Technology Indore, Indore, India*

[b] *Department of Biotechnology, Devi Ahilya Vishwavidyalaya*

E-mail: apurba.das@iiti.ac.in

† Electronic Supplementary Information (ESI) available: (1) TEM images of nanovesicles, nanocapsules and nanofibers; (2) AFM images of nanocapsules; (3) Fluorescence and optical microscope images; (4) Synthesis of peptide bolaamphiphile; (5) NMR spectra at different states (nanovesicles and nanofibers) and (6) Statistical analysis of MTT assay. See DOI: 10.1039/b000000x/

1. R. Ni, W. S. Childers, K. I. Hardcastle, A. K. Mehta and D. G. Lynn, *Angew. Chem. Int. Ed.*, 2012, **51**, 6635-6638.

2. S. Yuran, Y. Razvag and M. Reches, *Acs Nano,* 2012, **6**, 9559-9566.

3. C. Reiriz, R. J. Brea, R. Arranz, J. L. Carrascosa, A. Garibotti, B. Manning, J. M. Valpuesta, R. Eritja, L. Castedo and J. R. Granja, *J. Am. Chem. Soc.,* 2009, **131**, 11335-11337.

4. A. Montero, J. M. Beierle, C. A. Olsen and M. R. Ghadiri, *J. Am. Chem. Soc.,* 2009, **131**, 3033-3041.

5. S. Scanlon and A. Aggeli, *Nano Today,* 2008, **3**, 22-30.

6. S. Santoso, W. Hwang, H. Hartman and S. Zhang, *Nano Lett,* 2002*,* **2**, 687-691.

7. H. R. Marsden, J.-W. Handgraaf, F. Nudelman, N. A. J. M. Sommerdijk and A. Kros, *J. Am. Chem. Soc.,* 2010, **132**, 2370-2377.

8. J. B. Matson, C. J. Newcomb, R. Bitton and S. I. Stupp, *Soft Matter,* 2012, **8**, 3586-3595.

9. I. Maity, D. B. Rasale and A. K. Das, *Soft Matter,* 2012, **8**, 5301-5308.

10. E. Lee, J.-K. Kim and M. Lee, *Angew. Chem. Int. Ed.,* 2008, **47**, 6375-6378.

11. J. J. D. de Jong, L. N. Lucas, R. M. Kellogg, J. H. van Esch and B. L. Feringa, *Science,* 2004, **304**, 278-281.

12. M. D. Segarra-Maset, V. J. Nebot, J. F. Miravet and B. Escuder, *Chem. Soc. Rev.,* 2013, **42**, 7086-7098.

13. R. V. Ulijn and A. M. Smith, *Chem. Soc. Rev.*, 2008, **37**, 664-675.

14. T. Rehm and C. Schmuck, *Chem. Commun.*, 2008, 801-813.

15. K. H. Smith, E. Tejeda-Montes, M. Poch and A. Mata, *Chem. Soc. Rev.,* 2011, **40**, 4563-4577.

16. J. Kopecek and J. Yang, *Angew. Chem. Int. Ed.*, 2012, **51**, 7396-7417.

17. J. V. Georgieva, R. P. Brinkhuis, K. Stojanov, C. A. G. M. Weijers, H. Zuilhof, F. P. J. T. Rutjes, D. Hoekstra, J. C. M. van Hest and I. S. Zuhorn, *Angew. Chem., Int. Ed.,* 2012, **51**, 8339-8342.

18. J. Naskar, G. Palui and A. Banerjee, *J. Phys. Chem. B,* 2009, **113**, 11787-11792.

19. Y.-B. Lim, E. Lee, Y.-R. Yoon, M. S. Lee and M. Lee, *Angew. Chem. Int. Ed.,* 2008, **47**, 4525-4528.

20. N. S. Kehr, E. A. Prasetyanto, K. Benson, B. Ergun, A. Galstyan and H-J. Galla, *Angew. Chem. Int. Ed.,* 2013, **52**, 1156-1160.

21. C. A. DeForest and K. S. Anseth, *Angew. Chem. Int. Ed.,* 2012, **51**, 1816-1819.

22. M. J. Webber, J. Tongers, C. J. Newcomb, K.-T. Marquardt, J. Bauersachs, D. W. Losordo and S. I. Stupp, *Proc. Natl. Acad. Sci. U. S. A.,* 2011, **108**, 13438-13443.

23. B. Tian, J. Liu, T. Dvir, L. Jin, J. H. Tsui, Q. Qing, Z. Suo, R. Langer, D. S. Kohane and C. M. Lieber, *Nature Mater.,* 2012, **11**, 986-994.

24. D. Seliktar, *Science,* 2012, **336**, 1124-1128.

25. F. G. Omenetto and D. L. Kaplan, *Science,* 2010, **329**, 528-531.

26. A. R. Hirst, B. Escuder, J. F. Miravet and D. K. Smith, *Angew. Chem. Int. Ed.,* 2008, **47**, 8002-8018.

27. S. Roy, D. K. Maiti, S. Panigrahi, D. Basak and A. Banerjee, *RSC Adv*., 2012, **2**, 11053-11060.

28. H. Xu, A. K. Das, M. Horie, M. S. Shaik, A. M. Smith, Y. Luo, X. Lu, R. Collins, S. Y. Liem, A. Song, P. L. A. Popelier, M. L. Turner, P. Xiao, I. A. Kinloch and R. V. Ulijn, *Nanoscale,* 2010, **2**, 960-966.

29. C. Whitehouse, J. Fang, A. Aggeli, M. Bell, R. Brydson, C. W. G. Fishwick, J. R. Henderson, C. M. Knobler, R. W. Owens, N. H. Thomson, D. A. Smith and N. Boden, *Angew. Chem. Int. Ed.*, 2005, **44**, 1965-1968.

30. T. H. Larsen, M. C. Branco, K. Rajagopal, J. P. Schneider and E. M. Furst, *Macromolecules,* 2009, **42**, 8443-8450.

31. I. Maity, D. B. Rasale and A. K. Das, *RSC Adv.*, 2013, **3**, 6395-6400.

32. D. J. Pochan, J. P. Schneider, J. Kretsinger, B. Ozbas, K. Rajagopal and L. Haines, *J. Am. Chem. Soc.,* 2003, **125**, 11802-11803.

33. A. Sanchez-Ferrer, V. K. Kotharangannagari, J. Ruokolainen and R. Mezzenga, *Soft Matter,* 2013, **9**, 4304-4311.

34. L. A. Haines, K. Rajagopal, B. Ozbas, D. A. Salick, D. J. Pochan and J. P. Schneider, *J. Am. Chem. Soc.,* 2005, **127,** 17025-17029.

35. D. W. P. M. Lowik, E. H. P. Leunissen, M. van den Heuvel, M. B. Hansen and J. C. M. van Hest, *Chem. Soc. Rev.,* 2010, **39**, 3394-3412.

36. T. Yucel, C. M. Micklitsch, J. P. Schneider and D. J. Pochan, *Macromolecules,* 2008, **41,** 5763-5772.

37. Z. Yang, G. Liang and B. Xu, *Acc. Chem. Res.*, 2008, **41**, 315-326.

38. J. Hu, G. Zhang and S. Liu, *Chem. Soc. Rev.,* 2012, **41**, 5933-5949.

39. D. B. Rasale, I. Maity and A. K. Das, *RSC. Adv.,* 2012, **2**, 9791-9794.

40. A. K. Das, R. Collins and R. V. Ulijn, *Small,* 2008, **4***,* 279-287.

41. S. Ray, A. K. Das and A. Banerjee, *Chem. Mater.,* 2007**, 19***,* 1633-1639.

42. A. Aggeli, M. Bell, L. M. Carrick, C. W. G. Fishwick, R. Harding, P. J. Mawer, S. E. Radford, A. E. Strong and N. Boden, *J. Am. Chem. Soc.,* 2003, **125**, 9619-9628.

43 H. Shao and J. R. Parquette, *Angew. Chem. Int. Ed.*, 2009, **48**, 2525-2528.

44. E.T. Pashuck and S. I. Stupp, *J. Am. Chem. Soc.,* 2010, **132**, 8819-8821.

45. J. W. Sadownik, J. Leckie and R. V. Ulijn, *Chem. Commun.,* 2011, **47**, 728-730.

46. J. K. Sahoo, S. K. M. Nalluri, N. Javid, H. Webb and R. V. Ulijn, *Chem. Commun.,*2014, **50**, 5462-5464.

47. J. Gao, H. Wang, L. Wang, J. Wang, D. Kong and Z. Yang, *J. Am. Chem. Soc.,* 2009, **131**, 11286-11287.

48. T. Shimizu, M. Masuda and H. Minamikawa, *Chem. Rev.,* 2005, **105**, 1401-1443.

49. R. Djalali, J. Samson and H. Matsui, *J. Am. Chem. Soc.,* 2004, **126**, 7935-7939.

50. T. Wang, J. Jiang, Y. Liu, Z. Li and M. Liu, *Langmuir,* 2010, **26**, 18694-18700.

51. N. Krall, J. Scheuermann and D. Neri, *Angew. Chem. Int. Ed.,* 2013, **52**, 1384-1402.

52. F. von Nussbaum, M. Brands, B. Hinzen, S. Weigand and D. Habich, *Angew. Chem. Int. Ed.,* 2006, **45**, 5072-5129.

53. A. Kwiatkowska, F. Couture, C. Levesque, K. Ly, R. Desjardins, S. Beauchemin, A. Prahl, B. Lammek, W. Neugebauer, Y. L. Dory and R. Day, *J. Med. Chem.,* 2014, **57**, 98-109.

54. A. Baral, S. Roy, A. Dehsorkhi, I. W. Hamley, S. Mohapatra, S. Ghosh and A. Banerjee, *Langmuir,* 2014, **30**, 929-936.

55. D. Ke, C. Zhan, A. D. Q. Li and J. Yao, *Angew. Chem. Int. Ed.,* 2011, **50**, 3715-3719.

56. S. Ghosh, M. Reches, E. Gazit and S. Verma, *Angew. Chem. Int. Ed.,* 2007, **46**, 2002-2004.

57. D. B. Rasale, I. Maity, M. Konda and A. K. Das, *Chem. Commun.,* 2013, **49**, 4815-4817.

58. P. P. Bose, A. K. Das, R. P. Hegde, N. Shamala and A. Banerjee, *Chem. Mater.,* 2007, **19***,* 6150-6157.

59. K. Sun, K. Chen, G. Xue, J. Cai, G. Zou, Y. Li and Q. Zhang, *RSC Adv.,* 2013, **3**, 23997-24000.

60. J. T. Pelton and L. R. McLean, *Anal. Biochem.,* 2000, **277**, 167-176 .

61. S. Datta, S. K. Samanta and S. Bhattacharya, *Chem. Eur. J.,* 2013, **19**, 11364-11373.

62. X. Yan, Y. Cui, Q. He, K. Wang and J. Li, *Chem. Mater.,* 2008, **20***,* 1522-1526.

63. I. Maity, M. K. Manna, D. B. Rasale and A. K. Das, *ChemPlusChem.,* 2014, **79**, 413-420.

64. K. L. Morris, S. Zibaee, L. Chen, M. Goedert, P. Sikorski and L. C. Serpell, *Angew. Chem. Int. Ed.,* 2013, **125**, 2335-2339.

65. J. Naskar and A. Banerjee, *Chem. Asian J.,* 2009, **4**, 1817-1823.

66. V. Jayawarna, M. Ali, T. A. Jowitt, A. F. Miller, A. Saiani, J. E. Gough and R. V. Ulijn, *Adv. Mater.,* 2006, **18**, 611-614.

67. Y. Kuang and B. Xu, *Angew. Chem. Int. Ed.,* 2013, **52**, 6944-6948.

68. H. S. Parmar and A. Kar, *J. Med. Food.,* 2008, **11**, 376-81.

69. H. S. Parmar and A. Kar, *Drug Discov. Ther.,* 2009, **3,** 49-55.

70. A. Sethi, H. S. Parmar and A. Kumar, *Basic Clin. Pharmacol. Toxicol.,* 2011, **108,** 371-377.

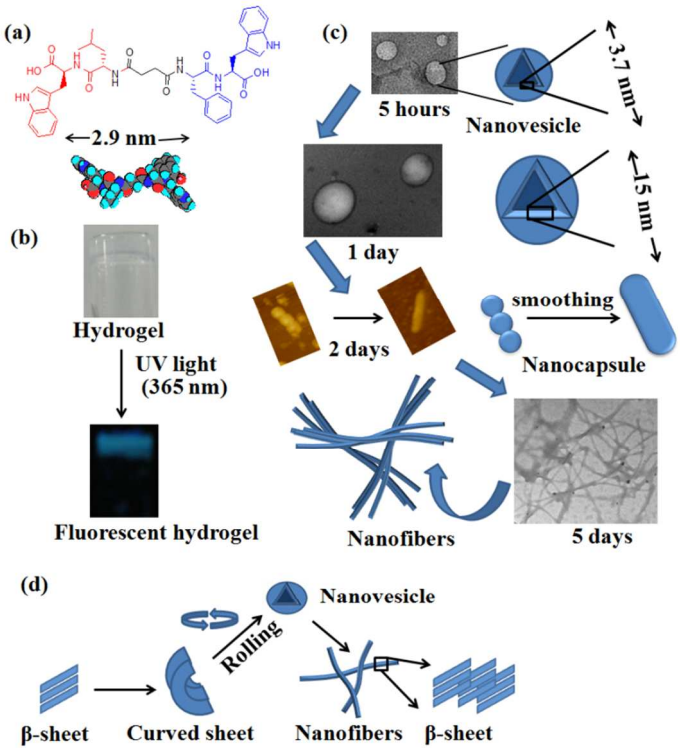

Scheme 1. (a) Molecular structure of peptide bolaamphiphile, (b) the self-supporting peptide bolaamphiphile hydrogel under day light which emits blue light upon the irradiation at 365 nm UV light, (c) self-programmed morphological transformation from nanovesicles to nanofibers through a third polymorphic capsular nanostructures and (d) the scheme represents the formation of β-sheets, which form vesicle via rolling up the sheet and then nanofibers are formed via reorientation of β-sheets.

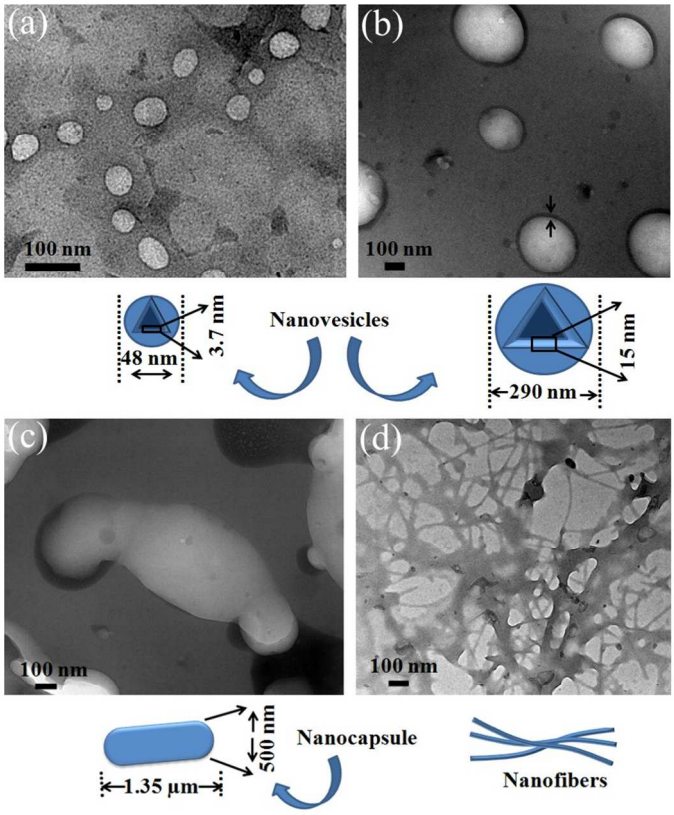

Fig. 1 TEM images show the nanostructural evolution of (a) nanovesicles at 5 hours, (b) multilayered nanovesicles at 1 day, (c) nanocapsules at 2 days and (d) nanofibrillar structures at 5 days of hydrogelation.

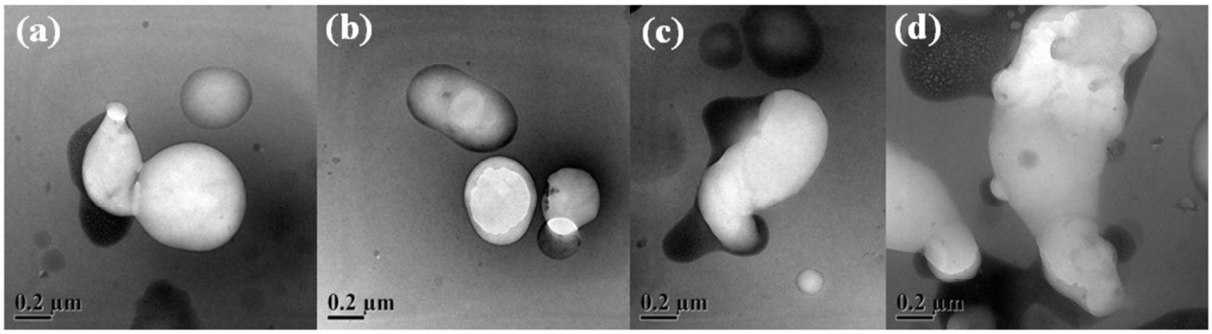

Fig. 2 TEM images show the formation of nanocapsules from the association of nanovesicles. TEM images show the (a) association of two vesicles towards formation of a nanocapsule, (b), (c) and (d) show the self-assembled peptide bolaamphiphile nanocapsules at 2 days.

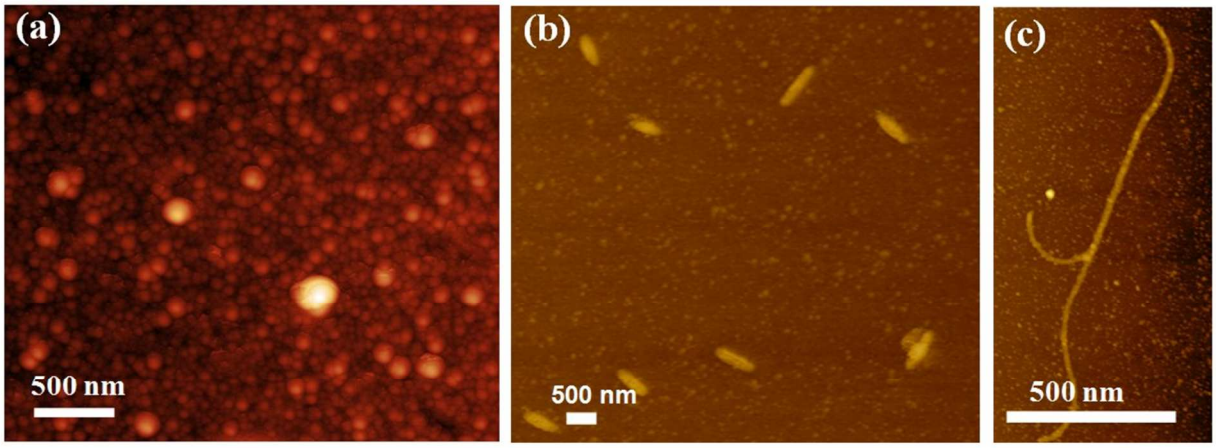

Fig. 3 AFM images show the nanostructural evolution of (a) nanovesicles at 1 day, (b) nanocapsules at 2 days and (c) nanofibrillar structures at 5 days of hydrogelation.

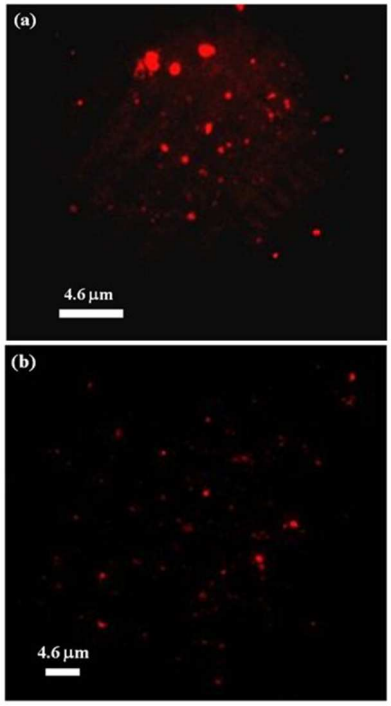

Fig. 4 Fluorescence microscopic images clearly show the encapsulation of a physiological dye, Congo red, by nanovesicles.

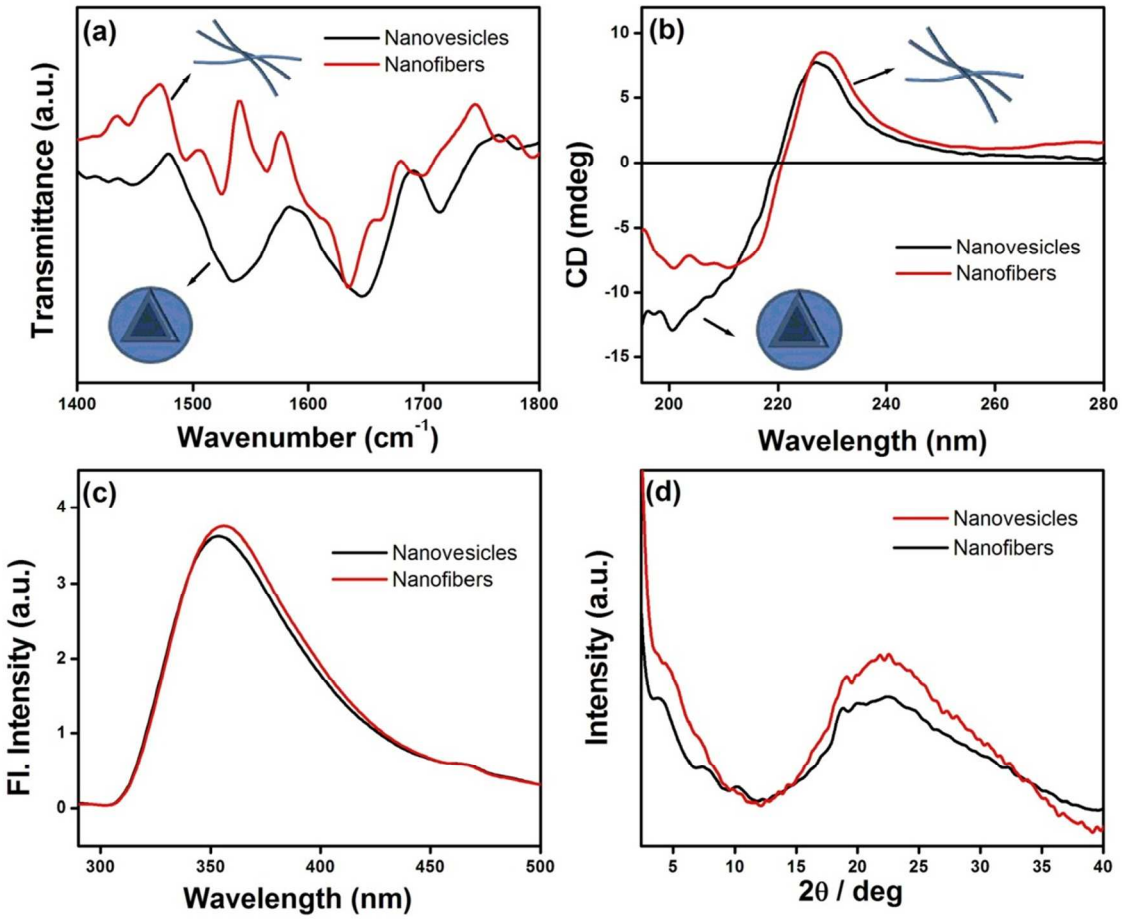

Fig. 5 (a) FTIR, (b) CD and (c) fluorescence spectra (concentration: 10 mmol L^{-1}, λ_{ex} = 280 nm) for both the nanostructures of nanovesicles and nanofibers. The spectroscopic studies confirm the more compact β-sheet arrangements inside the nanofibers rather than nanovesicles through the synergistic effect of hydrogen bonding and π-π stacking interactions. (d) PXRD for both the nanovesicles and nanofibers confirms the loose molecular arrangement inside the nanovesicles and more compact molecular arrangement inside the nanofibers.

Table 1. Evaluation of hydrogel preparation on cell viability and proliferation using MTT (3-[4,5-dimethylthiazol-2-yl]-2,5-diphenyl tetrazolium bromide) cell assay

Percentage viability as compare to control	% of hydrogel
77.983 ± 2.608^{aa}	10
91.126 ± 2.310^{bb}	20
99.69 ± 1.862^{bb}	30
126.293 ± 1.184^{cc}	40
197.126 ± 4.063^{dd}	50
95.82 ± 2.263^{be}	60
93.26 ± 1.330^{be}	70
92.656 ± 2.343^{be}	80
49.843 ± 1.222^{ff}	90
35.47 ± 1.102^{gg}	100

Values are the mean ± SE of three measurements. Means in columns without letters in common differ significantly ($P \leq 0.05$).

Table of Contents

Self-programmed nanovesicle to nanofiber transformation of a dipeptide appended bolaamphiphile and it's dose dependent cytotoxic behaviour

Indrajit Maity,[a] Hamendra S. Parmar,[b] Dnyaneshwar B. Rasale,[a] and Apurba K. Das*[a]

Self-programmed morphological transformation is achieved from a fluorescent peptide bolaamphiphile hydrogel. Nanostructural transition occurs from nanovesicles to nanofibers through an intermediate polymorphic state of nanocapsule morphology. Peptide bolaamphiphiles self-assembled into more ordered compact β-sheets from the early evolved loose molecular arrangements through the structural continuity of the β-sheet structures. Furthermore, the bolaamphiphile shows dose dependent behaviour towards cytotoxicity and cell-proliferation.